C h a p t e r   7

BULK METALLIC GLASSES WITH BENCHMARK THERMOPLASTIC PROCESSABILITY

The exceptional processability and large supercooled liquid region of bulk amorphous metals makes them highly promising candidates for thermoplastic processing. We report a lightweight (ρ = 5.4 g/cc) quaternary glass-forming alloy, $Zr_{35}Ti_{30}Cu_{8.25}Be_{26.75}$, having the largest supercooled liquid region (ΔT = 159 K at 20 K/min heating rate) of any known bulk-glass-forming alloy. The alloy can be cast into fully amorphous rods of diameter ~ 1.5 cm. The undercooled liquid exhibits an unexpectedly high Angell Fragility of m = 65.6. Based on these features, it is demonstrated that this alloy exhibits "benchmark" characteristics for thermoplastic processing. We report results of mechanical, thermal, rheological, and crystallization (TTT-diagrams) studies on this new material. The alloy exhibits high yield strength and excellent fracture toughness, and a relatively high Poisson's ratio. Simple micro-replication experiments carried out in open air using relatively low applied pressures demonstrate superior thermoplastic processability for engineering applications.

7.1. Introduction

Over the last two decades, the unique properties of bulk metallic glasses (BMGs), such as high strength, high specific strength, large elastic strain limit, excellent wear, and corrosion resistances along with other remarkable engineering properties have made these materials of significant interest for science and industry [1-8]. Researchers have designed families of multi-component systems that form bulk amorphous alloys, [4-8] among which Zr- (Vitreloy series) [4] and Pt-based [7] BMGs have been utilized commercially to produce items including sporting goods, electronic casings, medical devices, and fine jewelries.

The unique advantages of injection molding, blow molding, micro-replication, and other thermoplastic technologies are largely responsible for the widespread uses of plastics such as polyethylene, polyurethane, PVC, etc., in a broad range of engineering applications. Powder Injection Molding (PIM) of metals represents an effort to apply similar processing to metals, but requires blending of the powder with a plastic binder to achieve net shape forming and subsequent sintering of the powder. Given suitable materials, thermoplastic forming (TPF) would be the method of choice for manufacturing of metallic glass components because TPF decouples the forming and cooling steps by processing glassy material at temperatures above the glass transition temperature (T_g) and below the crystallization temperature (T_x), followed by cooling to ambient temperature [9, 10]. Conventional die casting requires rapid quenching to bypass the crystallization nose which limits the ability to make high quality casts and to create parts with complex geometries. Unfortunately, among the published metallic glasses, only the expensive Pt-, [7] and Pd-

119

based [11, 12] glasses have shown good thermoplastic formability. Zr-based metallic glasses, especially the Vitreloy series, are much less expensive than Pt- and Pd-based alloys, and have exceptional GFA, but they are usually strong liquids and low processing viscosities are unattainable in the supercooled liquid region (SCLR) between T_g and T_x [13, 14]. Strain-rate effect on viscosity of amorphous alloys has been extensively studied [15, 16].

7.2. Experimental

Mixtures of elements of purity ranging from 99.9% to 99.99% were alloyed by induction melting on a water-cooled silver boat under a Ti-gettered argon atmosphere. Typically 5 g ingots were prepared. Each ingot was flipped over and re-melted at least three times in order to obtain chemical homogeneity. A Philips X'Pert Pro X-ray diffractometer and a Netzsch 404C differential scanning calorimeter (DSC) (performed at a constant heating rate 0.33 K/s) were utilized to confirm the amorphous natures and to examine the isothermal behaviors in the SCLR of these alloys. The viscosity of $Zr_{35}Ti_{30}Cu_{8.25}Be_{26.75}$ as a function of temperature in the SCLR was studied using a Perkin Elmer TMA7 in the parallel plate geometry as described by Bakke, Busch, and Johnson [17]. The measurement was done with a heating rate of 0.667 K/s, a force of 0.02 N, and an initial height of 0.3 mm. The viscosity and temperature-time-transformation (TTT) diagrams of $Zr_{35}Ti_{30}Cu_{8.25}Be_{26.75}$ at high temperatures were measured in a high vacuum electrostatic levitator (ESL) [18, 19]. For the viscosity measurements, the resonant oscillation of the molten drop was induced by an alternating current (AC) electric field while holding the sample at a preset temperature. Viscosity was calculated from the decay time constant of free oscillation that followed the excitation pulse. To determine the TTT curve, an electrostatically levitated molten (laser melting) droplet (~ 3 mm diameter) sample was cooled radiatively to a predetermined temperature, and then held isothermally until crystallization. The temperature fluctuations were within ± 2 K during the isothermal treatment.

7.3. Results and Discussions

An alloy optimal for TPF would have good glass-forming ability, low viscosity (high fragility) in the SCLR, a low processing temperature, and a long processing time at that temperature before crystallization. We studied Be-bearing Zr-Ti-based quaternary metallic glasses with compositions in the range of $60\% \leq Zr+Ti \leq 70\%$. We found that compared with Vitreloys ($Zr + Ti = 55\%$), T_g is lowered, the liquid becomes more fragile, and the SCLR is increased. Two composition regions were found with alloys that exhibit exceptional properties for TPF in the $Zr_aTi_bCu_cBe_d$ system. These were $a \approx b$ with $c \leq 12.5\%$, and $a \approx 5b$ with $d \geq 20\%$. DSC curves of three representative alloys are presented in Figure 7.1 and Figure 7.2. The alloys all exhibit a very large SCLR with a single sharp crystallization peak at which the alloy undergoes massive eutectic crystallization to a multiphase crystalline product.
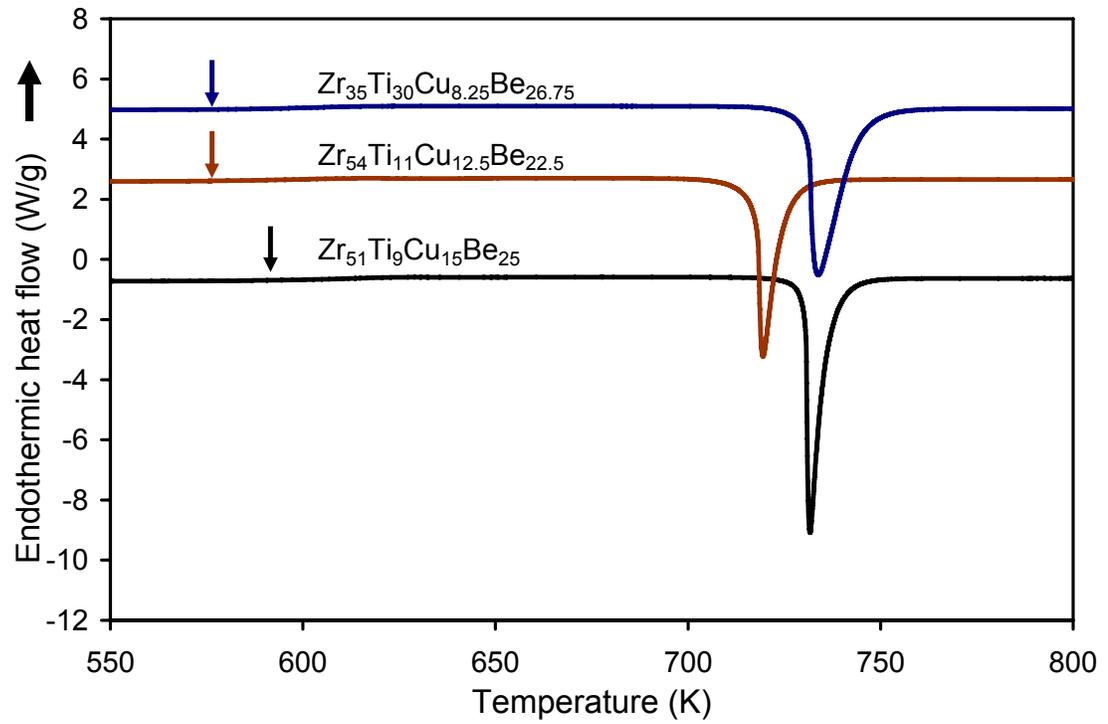
Figure 7.1. DSC scans of three typical metallic glasses with excellent glass-forming ability and extremely high thermal stability.
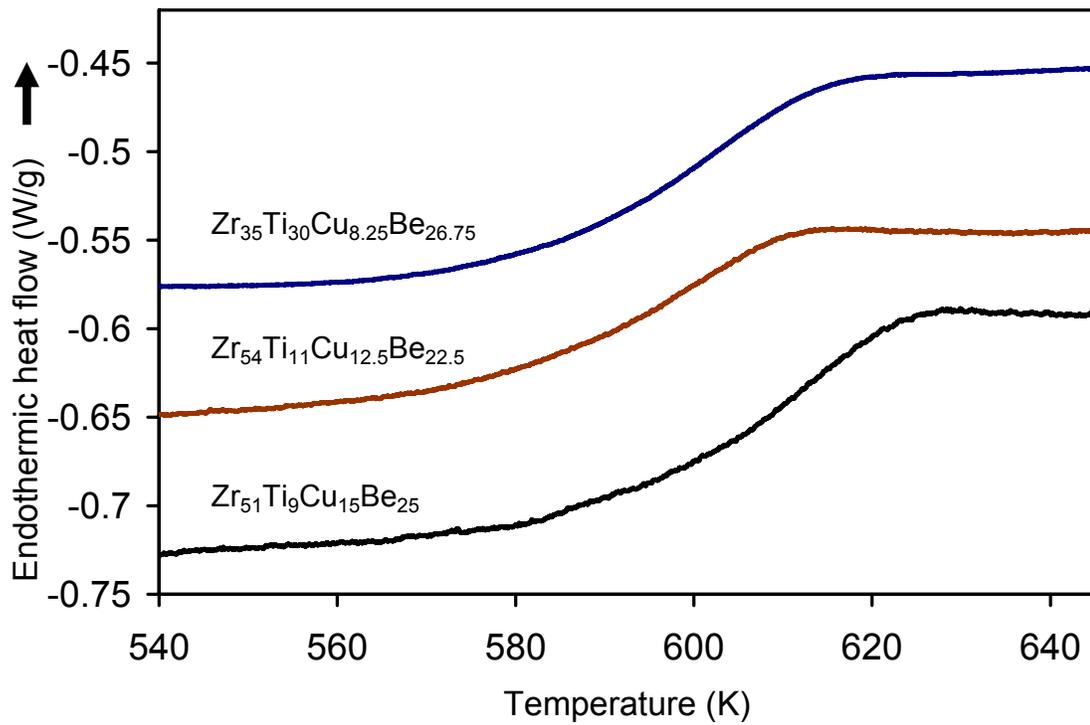
Figure. 7.2. A closer view of the glass transition temperatures of the three bulk metallic glasses.

The 5-g samples were generally found to freeze without any crystallization during preparation, resulting in a glassy ingot. The $Zr_{35}Ti_{30}Cu_{8.25}Be_{26.75}$ alloy can be cast into fully amorphous rods of diameter ~ 1.5 cm. The amorphous nature of all the samples studied in this work has been confirmed by X-ray diffraction. A summary of thermal properties of these BMGs are listed in Table 7.1 and compared with several earlier reported amorphous alloys [4, 5, 7, 11, 20-23]. The variations of SCLR, ΔT, ($\Delta T = T_x-T_g$, in which T_x is the onset temperature of the first crystallization event) and reduced glass-transition temperature T_{rg} ($T_{rg} = T_g/T_l$, where T_l is the liquidus temperature) are calculated. In the three newly designed alloys, $Zr_{35}Ti_{30}Cu_{8.25}Be_{26.75}$ exhibits the lowest T_g (578 K and about 45 K lower than that of Vitreloy1 or Vitreloy4) and the largest ΔT (159 K). It was further found that ΔT of the same glass can be enlarged to be 165 K by addition of 0.5 % Sn, giving the largest SCLR reported for any known bulk metallic glass.

In Figure 7.3 and Figure 7.4, the temperature dependence of equilibrium Newtonian viscosity of $Zr_{35}Ti_{30}Cu_{8.25}Be_{26.75}$ and several other metallic-glass-forming liquids with different Angell fragility numbers [24] are presented. The solid curve represents a Vogel-Fulcher-Tammann (VFT) fit to the viscosity data of $Zr_{35}Ti_{30}Cu_{8.25}Be_{26.75}$:

$$\eta = \eta_0 \exp(\frac{D^* \cdot T_0}{T - T_0}) \, ,$$

where η_0, D^*, and T_0 are fitting contants. T_0 is the VFT temperature and $\eta_0 \approx 10^{-5}$ Pa s. In the best fit, $T_0 = 422.6$ K and $D^* = 12.4$ are found, which yields an Angell fragility number of m = 65.6. Calculated from the empirical formula given by Wang et al. [25], we

obtain m = 56* T_g *$\Delta C_p(T_g)$/ ΔH_m = 67.0, where $\Delta C_p(T_g)$ = change in heat capacity at T_g = 0.414 J/g.K and ΔH_m = enthalpy of melting = 208.8 J/g. These values agree to each other within 2%.

The Angell fragility parameters of of $Zr_{35}Ti_{30}Cu_{8.25}Be_{26.75}$, Vitreloy series, Pd-based, and Pt-based metallic-glass-forming liquids [21, 26, 27] are listed in Table 7.1 as well. $Zr_{35}Ti_{30.}Cu_{8.25}Be_{26.75}$ shows rather fragile behavior compared with the strong Vitreloy series of liquids. Its viscosity in the thermoplastic zone is at least two orders of magnitude lower than that of Vitreloy 1 or Vitreloy 4 at the same temperature, and is comparable to that of Pd-based metallic glass. For example, the equilibrium viscosity at 410 °C for $Zr_{35}Ti_{30}Cu_{8.25}Be_{26.75}$ is measured to be only $6*10^4$ Pa.s, similar to that of viscous polymer melts [28]. As is known from the processing of thermoplastics, the formability is inversely proportional to viscosity. This alloy's low viscosity in the SCLR will result in a low Newtonian flow stress and high formability.

Table 7.1. Thermal, mechanical, and rheological properties of various BMG-forming alloys.

Materials	T_g (K)	T_x (K)	T_l (K)	ΔT (K)	T_g/T_l	T_{TPF}	m	S	$m \cdot \Delta T^*_{rx}$	G (GPa)	Y (GPa)	ν
$Zr_{51}Ti_9Cu_{15}Be_{25}$	592	730	1047	138	0.565	610~710	--	0.30	--	31.8	86.5	0.36
$Zr_{54}Ti_{11}Cu_{12.5}Be_{22.5}$	581	721	1035	140	0.561	600~700	--	0.31	--	30.3	82.8	0.37
$Zr_{35}Ti_{30}Cu_{8.25}Be_{26.75}$	578	737	1044	159	0.554	600~710	65.6	0.34	20.3	31.8	86.9	0.37
$Zr_{41.2}Ti_{13.8}Ni_{10}Cu_{12.5}Be_{22.5}$	623	712	993	89	0.627	640~690	49.9	0.24	7.98	35	95	0.35
$Zr_{46.75}Ti_{8.25}Ni_{10}Cu_{7.5}Be_{27.5}$	625	738	1185	113	0.527	650~710	44.2	0.20	10.0	35	95	0.35
$Pd_{43}Ni_{10}Cu_{27}P_{20}$	575	665	866	90	0.664	600~640	58.5	0.31	12.3	33	92	0.394
$Pt_{60}Ni_{15}P_{25}$	488	550	804	60	0.596	510~530	67.2	0.17	12.5	33.8	96.1	0.42
$Ce_{68}Cu_{20}Al_{10}Nb_2$	341	422	643	81	0.530	360~400	--	0.26	--	~11.5	~30.3	~0.313
$Au_{49}Ag_{5.5}Pd_{2.3}Cu_{26.9}Si_{16.3}$	401	459	644	58	0.623	420~440	--	0.24	--	26.5	74.4	0.406
$Pt_{57.5}Cu_{14.7}Ni_{5.3}P_{22.5}$	508	606	795	98	0.639	530~580	--	0.34	--	33.4	95.7	0.434
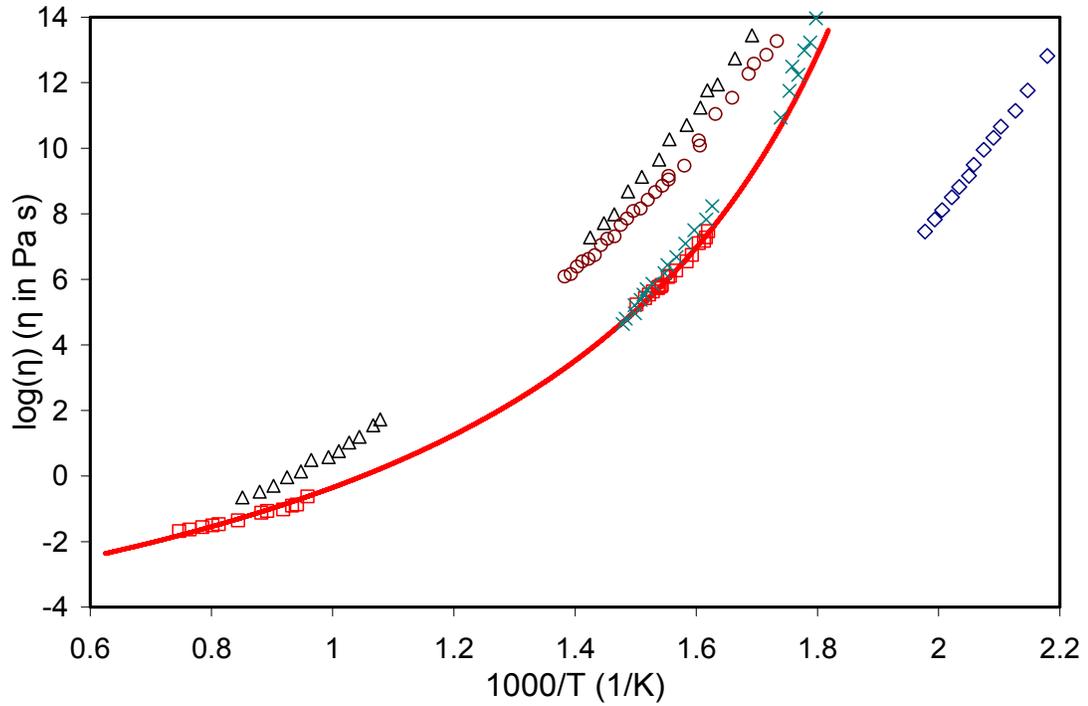
Figure 7.3. The temperature dependence of equilibrium viscosity of several metallic-glass-forming liquids: $Zr_{41.2}Ti_{13.8}Ni_{10}Cu_{12.5}Be_{22.5}$ (Vit1) (Δ); $Zr_{46.25}Ti_{8.25}Cu_{7.5}Ni_{10}Be_{27.5}$ (Vit4) (α); $Zr_{35}Ti_{30}Cu_{8.25}Be_{26.75}$ ($\square$); $Pd_{43}Ni_{10}Cu_{27}P_{20}$ ($\times$); and $Pt_{60}Ni_{15}P_{25}$ ($\Diamond$). It is shown that the viscosity of $Zr_{35}Ti_{30}Cu_{8.25}Be_{26.75}$ in the thermoplastic processing region (570 ~ 720 K) is at least two orders of magnitude lower than that of Vitreloy 1 or Vitreloy 4, and is comparable to Pd-based metallic glass and polymer glasses.
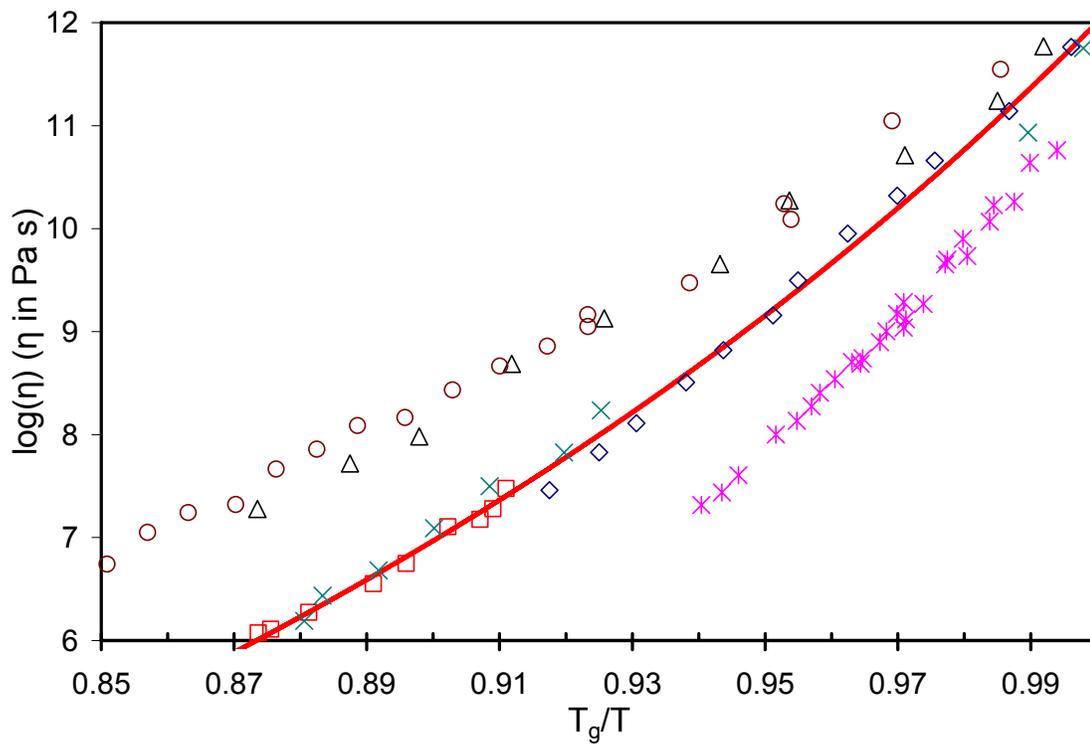
Figure 7.4. Angell fragility plot of several metallic-glass-forming liquids: $Zr_{41.2}Ti_{13.8}Ni_{10}Cu_{12.5}Be_{22.5}$ (Vit1) (Δ); $Zr_{46.25}Ti_{8.25}Cu_{7.5}Ni_{10}Be_{27.5}$ (Vit4) ($\maltese$); $Zr_{35}Ti_{30}Cu_{8.25}Be_{26.75}$ ($\square$); $Pd_{43}Ni_{10}Cu_{27}P_{20}$ ($\times$); $Pt_{60}Ni_{15}P_{25}$ ($\diamondsuit$); $Au_{77.8}Ge_{13.8}Si_{8.4}$ (*).

Recently, the normalized thermal stability, S [9], which is defined as $\Delta T / (T_l - T_g)$, was introduced to characterize the thermoplastic formability. As indicated in Table 7.1, $Zr_{35}Ti_{30}Cu_{8.25}Be_{26.75}$ demonstrates an S of 0.34, which is higher than that of all the other alloys and is as good as $Pt_{57.5}Cu_{14.7}Ni_{5.3}P_{22.5}$. Since S parameter is based on a oversimplified assumption of identical viscosity at T_l, a deformability parameter, $d^* = \log[\eta(T_g^*) / \eta(T_x)]$ [21] was also proposed and correlated with Angell fragility, m, and the reduced thermal stability, $\Delta T_{rx}^* = (T_x - T_g^*) / T_g^*$, where T_g^* is the glass transition temperature at which the viscosity is 10^{12} Pa s. Table 7.1 lists the calculated $m \cdot \Delta T_{rx}^*$ values for $Zr_{35}Ti_{30}Cu_{8.25}Be_{26.75}$, Vitreloy 1, Vitreloy 4, $Pd_{43}Ni_{10}Cu_{27}P_{20}$, and $Pt_{60}Ni_{15}P_{25}$ based on the measured viscosity data. It is seen clearly that $Zr_{35}Ti_{30}Cu_{8.25}Be_{26.75}$ shows the largest $m \cdot \Delta T_{rx}^*$, which implies a superior thermoplastic workability.

In Figure 7.5, we present the measured TTT curve for $Zr_{35}Ti_{30}Cu_{8.25}Be_{26.75}$ and other Vitreloy-series alloys [29]. The TTT curve indicates a nose shape, with the minimum crystallization time of ~ 3-10 s occurring somewhere between 700 K and 950 K. At 410 °C, where the equilibrium viscosity is on the order of 10^4 Pa s, a 600s thermoplastic processing window is indicated. To demonstrate the strong thermoplastic processability of the $Zr_{35}Ti_{30}Cu_{8.25}Be_{26.75}$ glassy alloy, we carried out plastic-forming experiments as shown in Figure 7.6 and Figure 7.7. The thermoplastic processing was done on a Tetrahedron hot press machine in the air at a pressure of 25 MPa with a processing time of 45 s, followed by a water-quenching step. Fig. 7.6 shows the microformed impression of a United States dime coin (Fig. 7.6 (b)) made on the surface of metallic glass wafers at ~ 370 °C (Fig. 7.6

(a)). Minimal oxidation was observed after the processing, which is consistent with the strong oxidation resistance of Be-bearing amorphous alloys. The final parts remain fully amorphous as verified by X-ray diffraction. It is found from the Rockwell hardness tests that no damage to the mechanical properties was caused by the thermoplastic processing. Before the TPF was carried out, we deliberately produced diamond-shape micro-indentation patterns (~ 100 μm) in the top flame of the dime using a Vickers hardness tester (Fig. 7.7 (a)). Figure 7.7 (b) presents the successfully replicated diamond pattern in the final part. Even the scratches (on the level of several μm) on the original dime are clearly reproduced. The results indicate a substantial advance in thermoplastic processing of amorphous metals.

The elastic constants of $Zr_{35}Ti_{30}Cu_{8.25}Be_{26.75}$ and several other BMGs are also shown in Table 7.1. Plenty of evidence suggests that a high Poisson's ratio is correlated with the ductile behavior of metallic glasses [30-35]. $Zr_{35}Ti_{30}Cu_{8.25}Be_{26.75}$ has a Poisson's ratio of ~ 0.37. The fracture toughness (K_{1C}) of $Zr_{35}Ti_{30}Cu_{8.25}Be_{26.75}$ was estimated to be ~ 85 MPa.m$^{1/2}$, while that of Vitreloy 1 is only ~ 20 ~ 45 MPa.m$^{1/2}$ [36-38]. The yield strength of $Zr_{35}Ti_{30}Cu_{8.25}Be_{26.75}$ under uniaxial compressive tests was found to be ~ 1.43 GPa. To design this new class of BMGs, a balance between strength and thermoplastic processablity has to be obtained. The present series of amorphous metals possesses superior thermoplastic formability at a low cost of strength and elastic energy storage.
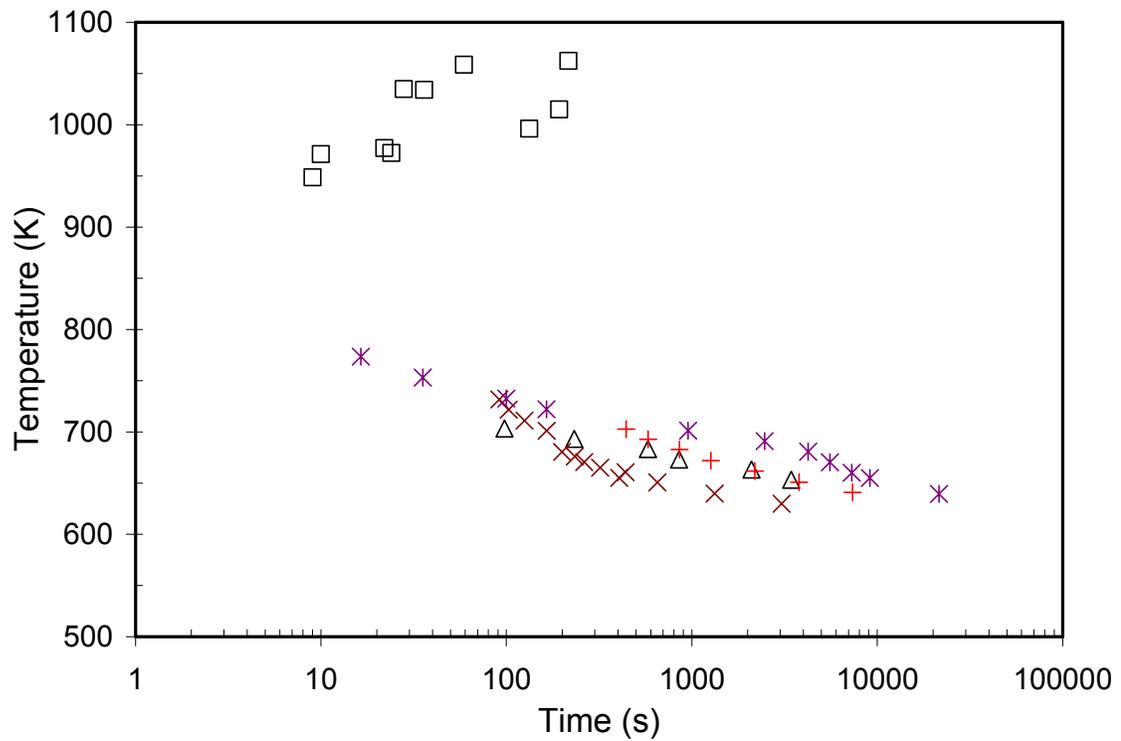
Figure 7.5. TTT diagrams for several amorphous alloys: $Zr_{41.2}$-$Ti_{13.8}Ni_{10}Cu_{12.5}Be_{22.5}$ (Vitreloy1) ($\times$); $Zr_{46.25}Ti_{8.25}Cu_{7.5}Ni_{10}Be_{27.5}$ (Vitre-loy4) ($*$); $Zr_{44}Ti_{11}Cu_{10}Ni_{10}Be_{25}$ (Vitreloy1b) ($+$); and the $Zr_{35}Ti_{30}$-$Cu_{8.25}Be_{26.75}$ alloy ($\square$ and Δ). The data are measured by electrostatic levitation ($\square$) and by processing in graphite crucibles (all the other data points), after heating from the amorphous state. At 410 °C, where the equilibrium viscosity is on the order of 10^4 Pa s, a 600s thermoplastic processing window is indicated.
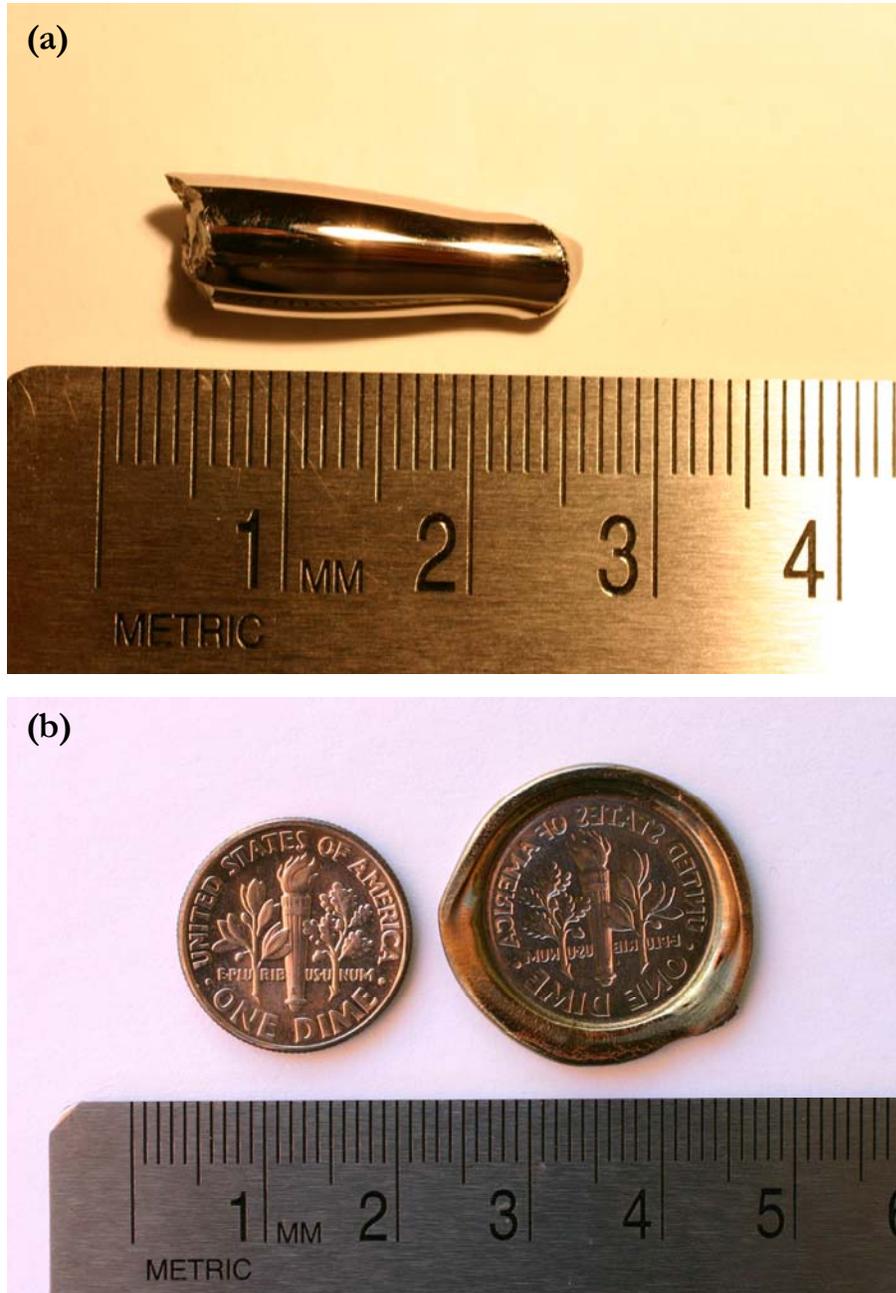
Figure 7.6. Demonstration of the strong thermoplastic processability of the $Zr_{35}Ti_{30}Cu_{8.25}Be_{26.75}$ metallic glass. It is the microformed impression of a United States dime coin made on the surface of metallic glass sheet processed at ~370 °C, indicating the excellent imprintability and viscous deformability. A diamond-shape micro-indentation pattern was successfully replicated in the final part as well.

133

(a)

Caltech   30μm*   Mag = 1.00 K X   EHT = 20.00 kV   WD = 34 mm   Signal A = SE2   Date :10 Jan 2007

(b)

Caltech   20μm*   Mag = 1.00 K X   EHT = 20.00 kV   WD = 34 mm   Signal A = SE2   Date :10 Jan 2007
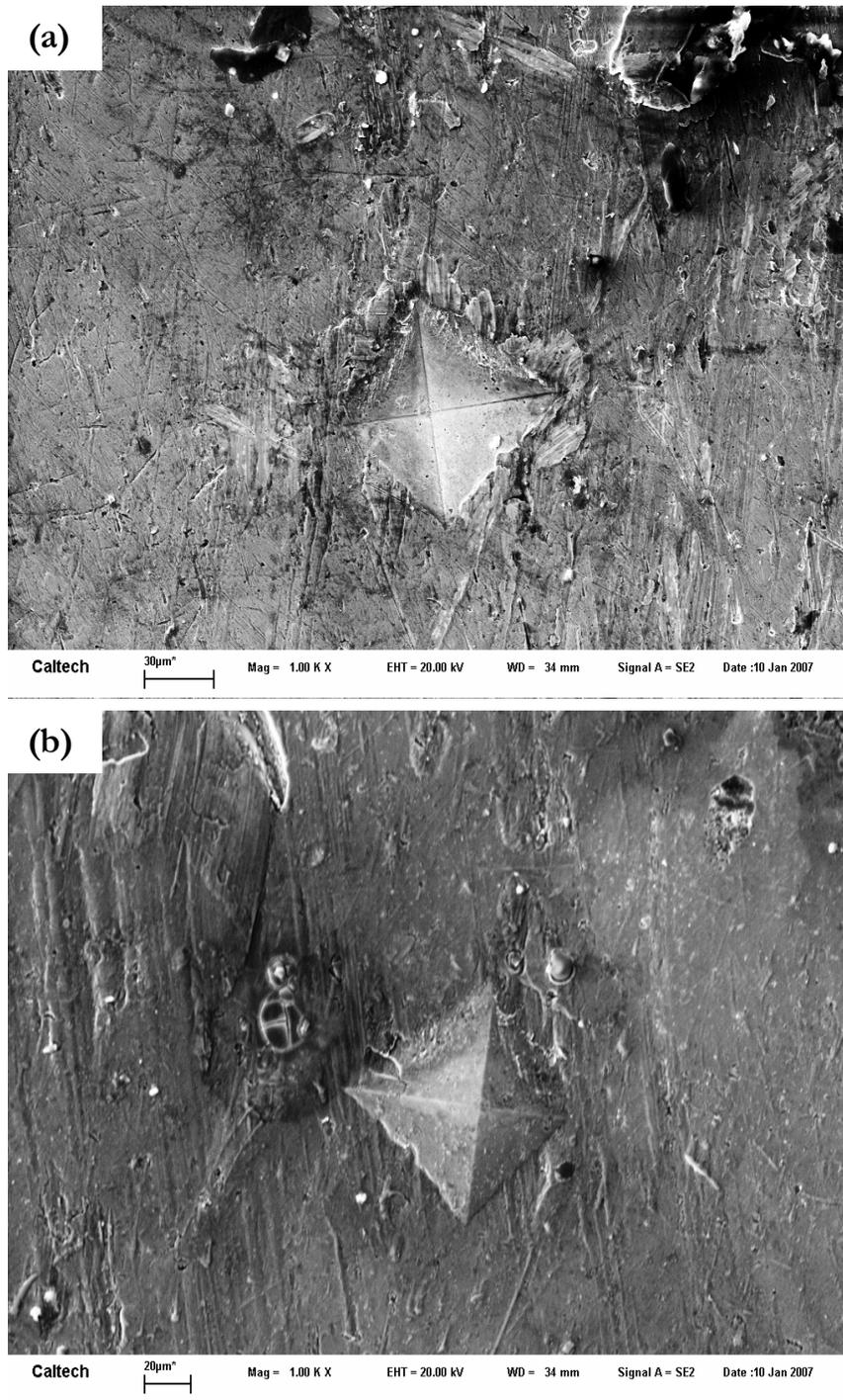
Figure 7.7. Demonstration of the strong thermoplastic processability of the $Zr_{35}Ti_{30}Cu_{8.25}Be_{26.75}$ metallic glass. A diamond-shape micro-indentation pattern was successfully replicated in the final part.

134

7.4. Chapter Concluding Remarks

In summary, we have designed a series of metallic-glass-forming alloys, having the combination of preferable properties for TPF, such as extraordinarily low viscosity in the thermoplastic zone, exceptional thermal stability, very low T_g, and excellent GFA. These alloys have demonstrated strong thermoplastic processability and excellent mechanical properties. We expect that this discovery will greatly broaden the engineering applications of amorphous metals by taking advantage of the unique properties of the newly designed BMGs.

References

[1] A. L. Greer, Science 267, 1947 (1995).

[2] W. L. Johnson, MRS Bulletin 24, 42 (1999).

[3] A. Inoue, Acta Materialia 48, 279 (2000).

[4] A. Peker and W. L. Johnson, Applied Physics Letters 63, 2342 (1993).

[5] B. Zhang, D. Q. Zhao, M. X. Pan, et al., Physical Review Letters 94 205502 (2005).

[6] V. Ponnambalam, S. J. Poon, and G. J. Shiflet, Journal of Materials Research 19, 1320 (2004).

[7] J. Schroers and W. L. Johnson, Applied Physics Letters 84, 3666 (2004).

[8] Z. P. Lu, C. T. Liu, J. R. Thompson, et al., Physical Review Letters 92 245503 (2004).

[9] J. Schroers, Jom 57, 35 (2005).

[10] J. Schroers and N. Paton, Advanced Materials & Processes 164, 61 (2006).

[11] G. J. Fan, H. J. Fecht, and E. J. Lavernia, Applied Physics Letters 84, 487 (2004).

[12] J. P. Chu, H. Wijaya, C. W. Wu, et al., Applied Physics Letters 90 034101 (2007).

[13] A. Masuhr, T. A. Waniuk, R. Busch, et al., Physical Review Letters 82, 2290 (1999).

[14] R. Busch and W. L. Johnson, Applied Physics Letters 72, 2695 (1998).

[15] F. Spaepen, Acta Metallurgica 25, 407 (1977).

[16] J. Lu, G. Ravichandran, and W. L. Johnson, Acta Materialia 51, 3429 (2003).

[17] E. Bakke, R. Busch, and W. L. Johnson, Applied Physics Letters 67, 3260 (1995).

[18] S. Mukherjee, J. Schroers, Z. Zhou, et al., Acta Materialia 52, 3689 (2004).

[19] S. Mukherjee, Z. Zhou, J. Schroers, et al., Applied Physics Letters 84, 5010 (2004).

[20] T. A. Waniuk, J. Schroers, and W. L. Johnson, Applied Physics Letters 78, 1213 (2001).

[21] H. Kato, T. Wada, M. Hasegawa, et al., Scripta Materialia 54, 2023 (2006).

[22] K. Shibata, T. Higuchi, A. P. Tsai, et al., Progress of Theoretical Physics Supplement, 75 (1997).

[23] J. Schroers, B. Lohwongwatana, W. L. Johnson, et al., Applied Physics Letters 87 061912 (2005).

[24] L. M. Martinez and C. A. Angell, Nature 410, 663 (2001).

[25] L. M. Wang, C. A. Angell, and R. Richert, Journal of Chemical Physics 125 (2006).

[26] V. N. Novikov and A. P. Sokolov, Physical Review B 74 064203 (2006).

[27] D. N. Perera, Journal of Physics-Condensed Matter 11, 3807 (1999).

[28] F. W. Billmeyer, *Textbook of Ploymer Science*, 1984.

[29] T. Waniuk, J. Schroers, and W. L. Johnson, Physical Review B 67 184203 (2003).

[30] H. S. Chen, J. T. Krause, and E. Coleman, Journal of Non-Crystalline Solids 18, 157 (1975).

[31] V. N. Novikov and A. P. Sokolov, Nature 431, 961 (2004).

[32] J. Schroers and W. L. Johnson, Physical Review Letters 93 255506 (2004).

[33] W. L. Johnson and K. Samwer, Physical Review Letters 95 195501 (2005).

[34] X. J. Gu, A. G. McDermott, S. J. Poon, et al., Applied Physics Letters 88 211905 (2006).

[35] J. J. Lewandowski, W. H. Wang, and A. L. Greer, Philosophical Magazine Letters 85, 77 (2005).

[36] J. J. Lewandowski, M. Shazly, and A. S. Nouri, Scripta Materialia 54, 337 (2006).

[37] P. Lowhaphandu and J. J. Lewandowski, Scripta Materialia 38, 1811 (1998).

[38] J. J. Lewandowski, Materials Transactions 42, 633 (2001).